Resonant x-ray scattering from the 4*p* quadrupole moment in YVO_3

T. A. W. Beale,[1] R. D. Johnson,[1] Y. Joly,[2] S. R. Bland,[1] P. D. Hatton,[1,*] L. Bouchenoire,[3] C. Mazzoli,[3] D. Prabhakaran,[4] and A. T. Boothroyd[4]

[1]*Department of Physics, University of Durham, Rochester Building, South Road, Durham DH1 3LE, United Kingdom*

[2]*Institut Néel, CNRS and Université Joseph Fourier, BP 166, F-38042 Grenoble 09, France*

[3]*European Synchrotron Radiation Facility, Boîte Postal 220, F-38043 Grenoble Cedex, France*

[4]*Department of Physics, Clarendon Laboratory, University of Oxford, Parks Road, Oxford OX1 3PU, United Kingdom*

(Received 8 February 2010; revised manuscript received 4 May 2010; published 21 July 2010)

We show that resonant scattering signals at the Bragg forbidden positions in YVO_3 originate from the anisotropic nature of the atomic scattering factor. The E1-E1 scattering from the electric-quadrupole moment is explained entirely through the crystal structure and does not require sensitivity to 3*d* orbital order. Simulations of the resonance using the FDMNES code suggest that the Jahn-Teller distortion provides an insignificant contribution to the intensity of the forbidden reflection. Thus we show that resonant x-ray diffraction at the vanadium *K*-edge in YVO_3 is largely insensitive, even indirectly, to 3*d* orbital order through Jahn-Teller distortions.

DOI: 10.1103/PhysRevB.82.024105 PACS number(s): 71.70.Ej, 61.05.cp, 78.20.Bh, 71.27.+a

I. INTRODUCTION

Understanding the interactions between different order parameters in transition-metal oxide systems is key to explaining their macroscopic behavior and subsequently of considerable interest. Scattering techniques have played a crucial role in unraveling these complex interactions, however, this can be complicated through conflicting interpretations.

In this paper we show resonant x-ray scattering[1] (RXS) results obtained from YVO_3, where reflections at (010) and (011) forbidden Bragg positions are observed to have a complex resonant spectrum. We show that these reflections and corresponding spectra can be explained purely by the anisotropic nature of the crystal structure and 4*p* states. As such, these reflections are not sensitive to the occupancy of the vanadium 3*d* orbitals.

YVO_3 and the rare-earth RVO_3 series form a family of pseudocubic vanadates showing similar behavior. The phase diagram[2] (Fig. 1) shows a number of different phase transitions, most notably the onset of orbital and magnetic order at low temperature. Of particular interest to this study is the subsequent lower temperature transition occurring in the systems with rare earths of a smaller ionic radius and with yttrium.

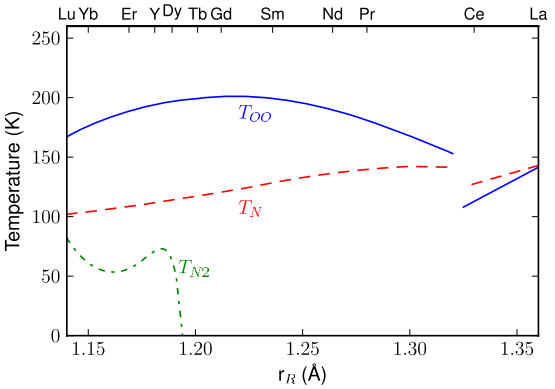

FIG. 1. (Color online) The phase diagram of RVO_3 over the entire region of the *R*-site ionic radius. Compounds with a smaller rare earth show a third transition below 100 K, where there is a change in the configuration of the spin and orbital order. Data from Miyasaka *et al.* (Ref. 2).

The magnetic structure of YVO_3 was first established by Kawano *et al.*,[3] who observed a transition into a *C*-type antiferromagnetic (AFM) structure at $T_{N1}=118$ K, followed by a lower temperature reorientation of the magnetic structure into *G*-type AFM structure at $T_{N2}=77$ K. This neutron-scattering study revealed a structural transition at T_{N2}, and the structural parameters were refined within the orthorhombic space group *Pbnm* in both phases. These details were then used by Sawada *et al.*,[4] who used first the generalized gradient approximation and then the local-density approximations (LDA)+*U* (Ref. 5) to model the magnetic structure. In order to stabilize the magnetic structures, specific orbital populations were required, with a *C*-type orbital order below T_{N2} and a change in the orbital order at the T_{N2} transition. Several unusual thermally induced magnetization reversals were also found in YVO_3.[6] In addition to an abrupt first-order magnetization reversal at T_{N2}, a gradual second-order reversal was observed at ~95 K. In consensus with Sawada and Terakura,[5] Ren *et al.*[6,7] proposed a change in the orbital order from *C*-type below T_{N2} to *G*-type above (Fig. 2) to explain the magnetization reversals.

Hartree-Fock calculations[8] indicate a strong coupling between the magnetic and orbital order, and the amount of $GdFeO_3$-type distortion (rotation of the VO_6 octahedra). Thus the relatively strongly distorted YVO_3 has a *G*-type AFM ground state below T_{N2} and the less distorted $LaVO_3$ has a *C*-type AFM structure below T_N. Above T_{N2} in YVO_3 the *C*-type AFM is favored by *G*-type orbital order with alternating orbitals along the *c* axis. The Jahn-Teller structural distortion associated with the *G*-type orbital order is incompatible with the *Pbnm* space group, and as such the discovery of a reduction in the space-group symmetry to monoclinic ($P2_1/b$) between 200 K (T_{OO}) and T_{N2}[9,10] was the first indirect experimental evidence of the orbital reorientation at T_{N2}. The optical and magneto-optical properties of YVO_3

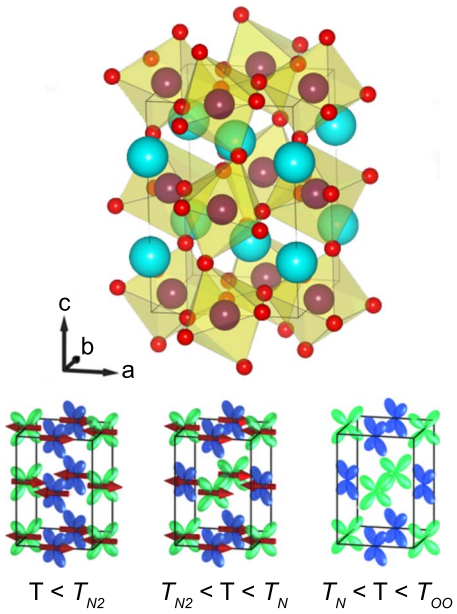

FIG. 2. (Color online) Top: the low-temperature crystal structure of YVO_3, with the yttrium in cyan, vanadium in purple in the center of the yellow VO_6 octahedra, and oxygen in red. The VO_6 octahedra clearly show the large crystal distortions in the material. Bottom: the reported orbital and magnetic structures of YVO_3 in the three phases below T_{OO} (Ref. 9).

were investigated with the aim of confirming the orbital structures.[11] These measurements were in agreement with the formation of orbital order, however, they were unable to positively confirm the orbital occupancy. The measurements did, however, confirm the lowering of the symmetry between T_{OO} and T_{N2}, suggesting either monoclinic $Pb11$ or triclinic $P\bar{1}$ space group.

Resonant x-ray scattering from forbidden reflections at the vanadium K-edge in YVO_3 was shown by Noguchi *et al.*[12] These resonances, although not fitted to any theoretical calculations, were attributed to the ordered occupancy of the $3d$ orbitals ($3d$-OO), due to the wave vector matching the expected orbital structure proposed by the LDA+U (Ref. 5) and Hartree-Fock[8] calculations. Such sensitivity was presumed to be caused by an induced electric quadrupole moment on the $4p$ states from the orbital occupancy in the $3d$ band. A coincidence of wave vector with the periodicity of the proposed $3d$-OO does not, however, prove that the measurement is directly probing the $3d$-OO. Similar claims were made in the manganite series,[13] which were then subsequently disputed, and it has become clear that these reflections originate from Jahn-Teller-type distortions.[14,15] Despite this insensitivity to $3d$-OO, the resonances at the transition metal K edges are a highly sensitive tool for observing crystallographic distortions. It has recently been shown that to be sensitive to $3d$-OO it is necessary to study resonant x-ray scattering at the $L_{2,3}$ edges.[16,17] This is difficult at the very soft (~500 eV) vanadium L edges as a very large periodic structure is required to observe a diffraction signal. As a result there have, as yet, been no reported soft x-ray resonant diffraction studies at the vanadium edges. Takahashi and Igarashi[18] modeled the K-edge resonant x-ray scattering data

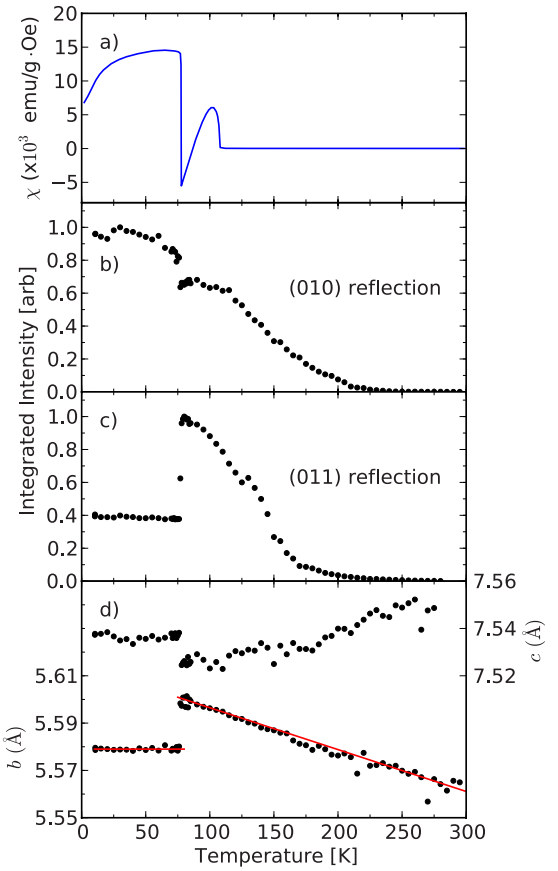

FIG. 3. (Color online) (a) Magnetization data from YVO_3 clearly showing the two magnetic phase transitions. Panels (b) and (c) show the temperature dependence of the intensity of (010) and (011) reflections. Panel (d) displays b and c lattice parameters, calculated through the position of (010) and (011) reflections.

from YVO_3 by Noguchi *et al.*,[12] using an *ab initio* band-structure calculation based on the LDA. Although their theoretical fits did not reproduce the experimental data perfectly, it provided compelling evidence that these scattering results arose mainly from the lattice distortion. We take this analysis further, measuring the K-edge RXS signal in more detail, and simulating these spectra using the FDMNES code.[19]

II. EXPERIMENTAL DETAILS

High quality single crystals of YVO_3 were grown at the University of Oxford using the floating zone method.[20] The magnetic transitions in the sample were confirmed with magnetization measurements using a SQUID magnetometer, where the sample was aligned such that the measurement was sensitive to the moment along the a axis. The measurement was taken through cooling from 300 to 2 K in an applied field of 10 Oe [Fig. 3(a)]. A crystal with dimensions ~5×5×5 mm^3 was aligned using a rotating anode diffractometer.[21] The sample of YVO_3 was prepared with two polished surfaces for diffraction, with (011) and (010) scattering vectors normal to the two surfaces.

Resonant x-ray diffraction experiments were performed on beamlines XMaS[22] and ID20.[23] The XMaS beamline is

situated on a bending magnet and ID20 on an insertion device at the ESRF. At both beamlines, a focused monochromatic x-ray beam was optimized with an incident energy of 5.49 keV, provided by a double bounce Si (111) monochromator with the higher energy x-ray harmonics rejected by a set of mirrors. The sample was mounted on a copper puck in a closed-cycle cryostat held in a Eulerian cradle. The sample was remounted for each reflection, such that the sample surface was close to normal to the scattering vector. Polarization analysis of the scattered beam was undertaken using a graphite (004) polarization analyzer crystal with a leakthrough at the vanadium K-edge of less than 0.5%.

Polarization analysis was further combined with a rotation of the sample around the scattering vector in order to measure the anisotropy of the signal through an azimuthal measurement. The intensity of the (010) reflection was measured through the rotation of the azimuthal axis (ϕ). Full linear polarization analysis[24,25] was undertaken at ID20 for the measurement of the (011) reflection above and below the phase transition T_{N2}. Using a 400 μm half-wave diamond phase plate the polarization of the incident beam was rotated, and a measurement was made of the polarization state of the scattered beam. The phase plate produced light with a measured 93% linear polarized component. This measurement technique avoids the necessity of a physical rotation of the sample and allows the experiment to be carried out at a particular geometry to minimize Renninger[26] (multiple) scattering.

III. RESULTS AND DISCUSSION

The YVO_3 crystal symmetry varies with temperature. At 295 K the space group is *Pbnm* with lattice parameters $a=5.277$ Å, $b=5.605$ Å, and $c=7.573$ Å. The *Pbnm* space group (equivalent through a cell choice to *Pnma*, No. 62), forbids the existence of (0, odd, 0) and (0, k, odd) reflections. Despite this, near the resonant condition, (011) and (010) reflections can be seen due to the local distortion around the resonating atom.

At energies far from the absorption edge, resonant scattering is negligible, and the forbidden reflections are not observed. The atomic scattering factor (ASF) is represented by a second-rank tensor that is determined by the crystal symmetry, that becomes non-negligible close to the absorption edge. At the forbidden reflections the scalar (charge) scatter from the E1-E1 dipole transition is not present, therefore we are able to observe the much weaker electric quadrupole through the same E1-E1 dipole ($1s-4p$) transition. As the scattering intensity is tensorial, rather than scalar in nature, it depends on the relative orientation of the anisotropy of the 4p valence states and the polarization vector of the x-ray beam. Thus information about these 4p states can be retrieved through azimuthal and polarization analysis.

This kind of scattering process has been seen many times previously, not only in vanadates but also in other transition-metal oxides such as manganites[13,27] and ferrates,[28,29] and is also known as Templeton scattering[30,31] or anisotropic tensor of susceptibility scattering.[28,29] Somewhat confusingly, the electric quadrupole has commonly been called orbital order. This is despite the fact that the electric-quadrupole moment on the 4p states is constrained by the local crystal structure around the vanadium and does not necessarily reflect the 3d electric quadrupole moment at the vanadium sites, i.e., the occupancy of the 3d orbitals. Moreover, the 4p band is delocalized, and as such is strongly influenced by the surrounding environment, rather than directly influenced by the localized 3d electrons. A direct probe of 3d-OO is possible through resonant x-ray scattering at the $L_{2,3}$ edges, however, this is not possible in YVO_3. Such information on the local structure may well provide, at best, constraints such that the 3d-OO can be inferred from the anisotropy of the 4p states. Sawada and Terakura[5] have shown using the LDA+U calculations that the crystal structure of YVO_3 (determining the anisotropy of the 4p states), is strongly linked to the orbital occupancy of the d orbitals, such that the orbitals extending along the long V-O bond pair are preferentially occupied.

Figure 3 shows the magnetization, intensity of (010) and (011) reflections, and lattice parameters of the sample calculated from the 2θ values of these reflections as a function of temperature. The magnetization data clearly shows two transitions at 118 K (T_{N1}) and 77 K (T_{N2}). These correspond to the two magnetic phase transitions into the high-temperature C-type magnetic structure and low-temperature G-type magnetic structure. T_{N2} corresponds to a structural change seen in the intensity of the reflections and discontinuity in the lattice parameters. The values for the c lattice parameter were extracted from the (011) position, using the b lattice-parameter values shown by the solid line in Fig. 3(d). Both reflections can be seen at room temperature, and there is a gradual increase in the intensity of the reflections below 200 K (T_{OO}). This measurement of the integrated intensity of the forbidden reflections is very different to that observed by Blake *et al.*,[9] where a much more abrupt, first-order like, transition was observed. Our results suggest a more gradual transition from the orthorhombic high-temperature phase above T_{OO}, to the monoclinic $P2_1/b$ (or lower) phase. This is supported through the near-linear change in the lattice parameters below 300 K, rather than an abrupt transition.

An extended transition is also observed in other RVO_3 crystals, including $GdVO_3$ where the monoclinic angle varies between 90.00° and 90.08° over 120 K.[32] No change in the intensity of either reflection in YVO_3 was seen at T_{N1}, showing that the onset of C-type magnetic order is not accompanied by a change in the crystal structure or the anisotropy of the 4p states.

Energy resonances of (010) and (011) reflections were measured at fixed wave vector. Calculating the ASF to simulate the resonant spectra is nontrivial. We have used the FDMNES code[19] using multiple-scattering theory, with the most recent crystallographic parameters from Reehuis *et al.*[33] as an input. Figure 4 (inset) shows the x-ray fluorescence spectra (XFS) from the sample in the vicinity of the vanadium K-absorption edge. This measurement is important, as the FDMNES calculation does not accurately predict the position of the edge in energy. For this reason x-ray absorption near-edge structure, or in this case XFS is used to calibrate this edge for the simulation.

Figures 4 and 5 show the diffraction resonant spectra at (011) and (010) reflections above and below T_{N2}. The solid

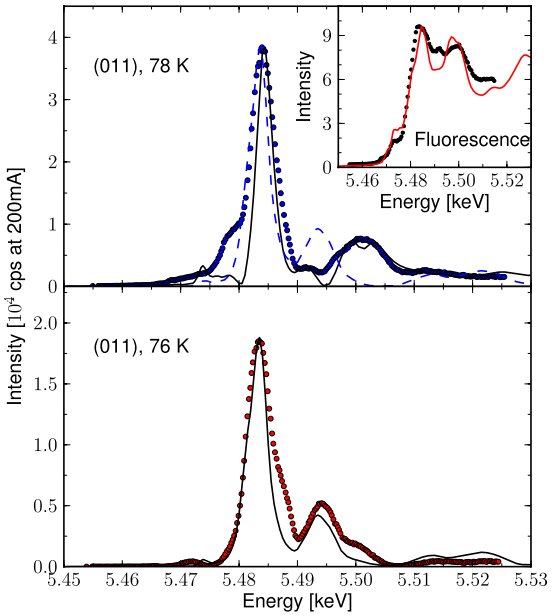

FIG. 4. (Color online) Fixed wave-vector energy scans through the (011) reflection above and below the magnetic transition, T_{N2}. The inset in the upper panel shows the fluorescence spectra from YVO_3 measured with an open detector far away from a diffraction signal. Experimental data are shown by filled circles with the FDMNES calculations shown by solid lines using the monoclinic $P2_1/b$ space group in the upper panel above the transition and the orthorhombic *Pbnm* space group in the lower panel, below T_{N2}. The dashed line in the upper panel is the FDMNES calculation using the orthorhombic *Pbnm* space group.

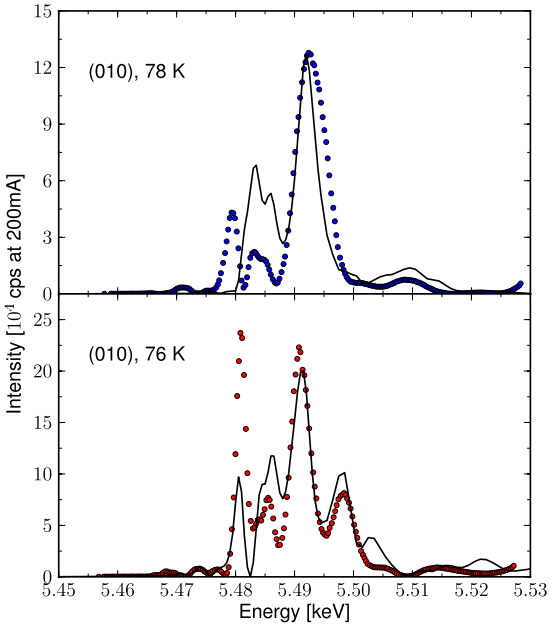

FIG. 5. (Color online) An energy scan at fixed wave vector through the V *K* edge of the (010) reflection at 76 and 78 K, either side of the magnetic transition T_{N2}. The solid lines show the calculations using the FDMNES using the *Pbnm* (below T_{N2}) and $P2_1/b$ (above T_{N2}) space groups.

lines on each are the results of the FDMNES calculations. In order to accurately recreate the change in the (011) spectrum above and below the transition, it was necessary to use the monoclinic space group $P2_1/b$ (Ref. 33) above T_{N2} and the orthorhombic space group below T_{N2}. A good agreement between the FDMNES calculation and both the (011) resonance and the XFS spectra was obtained using a cluster radius of 6.6 Å containing 115 atoms, with a Fermi energy of 4.8 eV below the vanadium absorption edge of 5.465 keV. The main features of the (010) reflection are also recreated, although the fit is less good than that of the (011). The deficient area of this simulation is the low energy pre-edge peaks. The general shape of the resonances agree with those measured by Noguchi *et al.*,[12] however, the higher flux in our measurements reveal more clearly the resonant details. A direct comparison can be made by the FDMNES calculations presented here, and the LDA calculations by Takahashi and Igarashi[18] In both calculations it is clearly the (010)-type reflection that provides a less satisfactory simulation of the data. The calculations shown in this paper give better agreement with the intensity of each part of the resonance than those by Takahashi. The shortcomings of the FDMNES simulations are likely to be due to a deficiency in the input structure. This could be a relatively small ionic movement changing the local environment of the vanadium ion, or a lowering of the crystal symmetry. One such possibility is the proposed dimerization of the vanadium ions along the *c* axis.[34,35]

By removing the Jahn-Teller distortion from the low-temperature *Pbnm* crystal structure, we re-ran the FDMNES calculations under otherwise identical conditions (Fig. 6). This demonstrates that the Jahn-Teller distortion plays an insignificant role in the diffraction spectra. As described above, the *d*-OO is strongly coupled to the length of the V-O bonds, i.e., the Jahn-Teller distortion. As the resonances, modeled by FDMNES, are unchanged with the removal of such a distortion we arrive at the conclusion that the (011) at the vanadium *K* edge is completely *insensitive* to the Jahn-Teller distortion, and the (010) has only a very small sensitivity to the Jahn-Teller distortion and therefore the orbital order. It should, however, be noted that the Jahn-Teller distortions are very small in YVO_3, and resonant *K*-edge scattering spectra in systems with a large Jahn-Teller distortion, such as $La_{0.5}Sr_{1.5}MnO_4$ may well provide an indirect probe of orbital order.

The FDMNES calculations are not able to fully explain the temperature dependencies of the reflections shown in Fig. 3. The calculated intensity of the (010) reflection stays largely constant with only a 20% reduction from the 85 K structure to the 295 K structure. Similarly, the intensity of the (011) reflection at 5 and 295 K are the same within 10%, however, there is a increase in the calculated intensity at 85 K, by a factor of four, in agreement with the sharp increase shown in Fig. 3(c). As such, FDMNES is unable to predict the gradual reduction in intensity seen between 100 and 250 K. FDMNES is a ground-state calculation and has no thermal parameters; different temperatures are simulated through their respective structures. At first inspection it appears that the reduction in intensity matches the decrease in the Jahn-Teller distortion,[9] thus it would be reasonable to assume that this causes the intensity reduction. However, the FDMNES calculation incorporates the Jahn-Teller distortion, as part of the crystal struc-

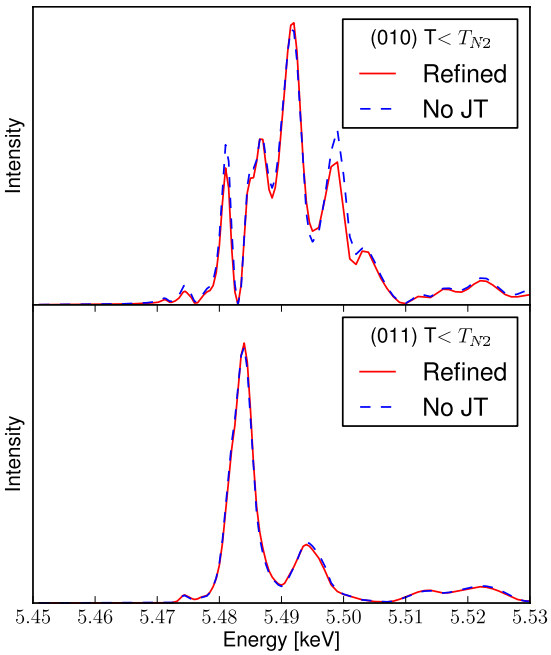

FIG. 6. (Color online) FDMNES calculations of the energy spectra at both reflections using the crystal structure as refined by Reehuis *et al.* (Ref. 33) in the *Pbnm* ($T<T_{N2}$) phase, and a modified crystal structure with no Jahn-Teller (No JT) distortion.

ture, and no reduction is shown in the calculation. Therefore the reduction in intensity is either due to a limitation in the intensity calculation of FDMNES or due to an order parameter not included in the calculation. Simultaneous to the reduction in the Jahn-Teller distortion is the disorder of the orbital order.[36] This, however, is predominantly confined to the 3*d* electronic states, with very little overlap between the 3*d* and 4*p* electron bands. The dipole 1*s*-4*p* transition excited through the resonant scattering process at the vanadium absorption edge is, however, not sensitive to the 3*d* bands.[37] Such 3*d*-electron correlations could be observed through the 1*s*-3*d* quadrupole transition as seen in V_2O_3.[38] If this was present it would be expected to be very weak in comparison to the dipole transition, and appear in the pre-edge. Such a quadrupole transition would also have a completely different azimuthal dependence. The azimuthal dependencies of the small features in the energy spectra at 5.475 keV (011) and 5.472, 5.474, 5.478 keV (010) were measured and found to have the same dependence as the main features, and are therefore part of the dipole spectra. As such, it is difficult to assign this temperature dependence to a correlation of the 3*d*-electron bands. Despite not being sensitive either to the 3*d*-electronic order, or the Jahn-Teller distortions, it is clear that the symmetry of the crystal undergoes a transition concomitant to the orbital order-disorder transition that we are sensitive to. Revealing the exact nature of this symmetry transition is currently beyond the capability of FDMNES.

The tensorial ASF describing the intensity of the reflection is dependent on the relative orientation of the electric-field polarization vectors and the crystal. Thus, a measurement of the symmetry of the vanadium 4*p* states can be made either by rotating the polarization of the incident beam or by rotating the sample while maintaining the Bragg condition,

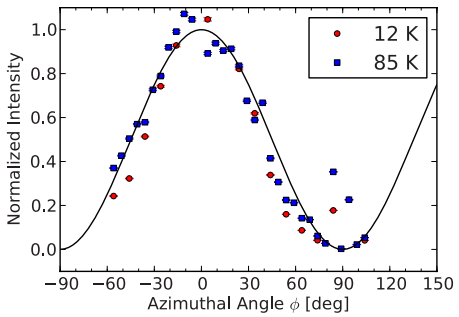

FIG. 7. (Color online) Integrated intensity of the azimuthal dependence of the (010) reflection at 12 and 85 K, measured with an incident x-ray energy of 5.492 keV. The azimuthal reference vector was [001], such that ϕ=0° corresponds to the (001) reflection in the beam direction. The reflection was present only in the rotated π polarization channel and shows the same dependence above and below T_{N2}. The solid line shows the calculated azimuthal dependence, which is identical in both phases.

i.e., rotating the crystal around the scattering vector.

A simulation of these measurements is dependent on the ASF tensor[39] that was calculated using the FDMNES code. By combining this tensor with the polarization states the intensity of the signal can be calculated for different geometries.[40] Both above and below the transition the (010) reflection was only observed in the rotated (σ-π') polarization channel, as predicted through our tensor analysis. In addition, there is no change to the azimuthal dependence of the (010) reflection above and below T_{N2} (Fig. 7). A calculation of the azimuthal dependence through deriving the scattering tensor in each space group[29] confirms that no change is expected at this wave vector. Despite the relative strength of the (010) reflection, the azimuthal measurement has significant random errors that are apparent from the spread of the data. These errors are difficult to quantify as the peak shape is very regular and consistent, leading to very low fitting errors (as shown in the data). Rather, the errors arise from the nature of the measurement, where the rotation of the sample slightly changes the sample position relative to the x-ray beam. This not only changes the footprint geometry but tracks the beam footprint across the sample illuminating slightly different quality areas of the sample. With the general trend of beam size reduction at new facilities, this problem will increase. In addition, this crystal structure supports a large amount of Renninger scattering that is highly dependent on the geometry of the experiment. Thus, as the crystal is rotated, contamination of the weak forbidden reflection through multiple scattering is common, and is seen close to 90° in both measurements.

The (011) reflection has a much more complex azimuthal measurement, with intensity in both polarization channels both above and below T_{N2}. Although an azimuthal measurement was obtained, the results were not satisfactory for determining any conclusions. A solution to this experimental difficulty is to rotate the incident polarization rather than the sample. In this way, an alignment free from multiple scattering can be selected, and throughout the measurement there is no change in the footprint of the x-ray beam. The experiment is not trivial, however. In order to rotate the incident light, a

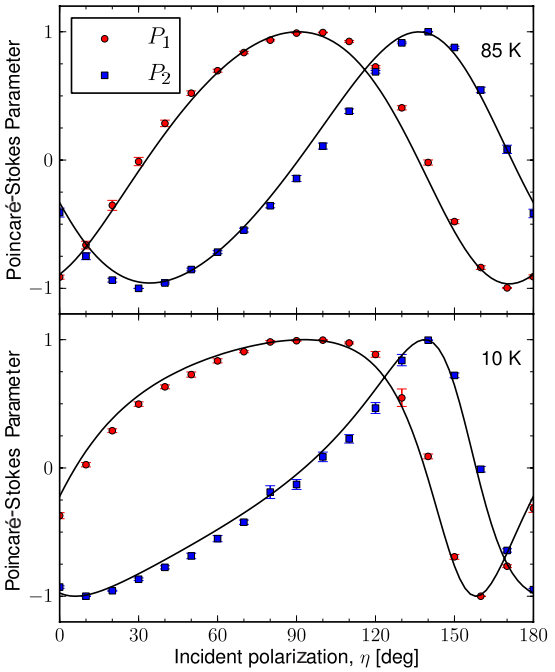

FIG. 8. (Color online) The Poincaré-Stokes' parameters P_1 and P_2, of the (011) reflection above (upper) and below (lower) the transition, measured through full linear polarization analysis, with an incident x-ray energy of 5.484 keV. With an azimuthal reference vector [100], the measurements were taken at $\phi=-78.6°$, a position selected for minimal Renninger scattering. The solid lines show the FDMNES calculated dependencies.

thin diamond crystal is used as a half-wave plate, the alignment of which is crucial to minimize nonlinearly polarized light. By rotating the phase plate in the incident beam, the polarization state of the beam is rotated. By analyzing the polarization state of the scattered beam with a range of incident polarization state, a "full linear polarization analysis"[25,41] of the signal can be measured. Figure 8 shows the dependence of the Poincaré-Stokes parameters P_1 and P_2 with the incident polarization angle (η) above and below T_{N2}, where $\eta=0$ corresponds to horizontally polarized (σ) incident x rays, and

$$P_1 = \frac{I_\sigma - I_\pi}{I_\sigma + I_\pi}, \quad P_2 = \frac{(I_{45°} - I_{-45°})}{(I_{45°} + I_{-45°})},$$

where I_σ (I_π) is the intensity of the x rays in the σ (π) polarization channel of the scattered beam, and $I_{+45°}$ $(I_{-45°})$ is the intensity of x rays polarized at +(−)45° from the horizontal. The detection of the polarization state was made through measuring the intensity of the beam polarized at increments of 18° between I_σ and $I_{-\sigma}$ then fitting this intensity variation with a cosine function. P_1 and P_2 were calculated from the offset of the cosine function from the origin.

The figure shows both experimental and FDMNES calculated dependencies from the tensor generated from the symmetry of the crystal structure. The FDMNES calculation for the 85 K data used the monoclinic $P2_1/b$ space group that was found to give a better agreement with the energy spectra. Both these calculations are direct outputs from the FDMNES code and have no "free" parameters to optimize. As such, it is astonishing that the agreement between this calculation and the data is so good. It has been suggested that the symmetry of YVO_3 between T_{OO} and T_{N2} is lower than $P2_1/b$,[11] however, there is no requirement to invoke this lower symmetry to agree with our data. Such good agreement of the simulation to both polarization and azimuthal dependencies confirm that the reflections are purely from the electric quadrupole, and there is no contribution either from the electric dipole or scalar-charge scattering.

IV. SUMMARY

The resonant scattering at the (011) and (010) forbidden reflection sites in YVO_3 can be explained purely through the crystal structure. Simulations of the resonant spectra with the FDMNES code using the crystal structure as an input show good agreement with the data. In order for the simulation to agree with the spectrum and the polarization dependence of the (011) reflection the symmetry of the intermediate phase was lowered from orthorhombic. Correspondingly simulations based on the monoclinic $P2_1/b$ space group as suggested by Reehuis *et al.*[33] show a good agreement with the data.

We have shown that these reflections are not sensitive to the Jahn-Teller distortions. This insensitivity is likely to be due to the extremely small Jahn-Teller distortion compared to the relatively large $GdFeO_3$ distortions of the system. As such, the scattering at (011) and (010) forbidden Bragg reflections arises from the anisotropy of the $4p$ states, however, we have shown that neither reflection is sensitive to Jahn-Teller distortions and therefore $3d$ orbital order, even indirectly.

ACKNOWLEDGMENTS

This work was performed on the EPSRC-funded XMaS beam line at the ESRF, directed by M. J. Cooper and C. Lucas. We are grateful to the beam line team of S. D. Brown, L. Bouchenoire, and P. Thompson for their invaluable assistance and to S. Beaufoy and J. Kervin for additional support. The crystal schematic shown in Fig. 2 was depicted using VESTA (Ref. 42). T.A.W.B., R.D.J., S.R.B., and P.D.H. wish to thank EPSRC and STFC for support.

*p.d.hatton@dur.ac.uk

[1] J. P. Hannon, G. T. Trammell, M. Blume, and D. Gibbs, Phys. Rev. Lett. **61**, 1245 (1988).
[2] S. Miyasaka, Y. Okimoto, M. Iwama, and Y. Tokura, Phys. Rev. B **68**, 100406(R) (2003).
[3] H. Kawano, H. Yoshizawa, and Y. Ueda, J. Phys. Soc. Jpn. **63**, 2857 (1994).
[4] H. Sawada, N. Hamada, K. Terakura, and T. Asada, Phys. Rev. B **53**, 12742 (1996).
[5] H. Sawada and K. Terakura, Phys. Rev. B **58**, 6831 (1998).
[6] Y. Ren, T. T. M. Palstra, D. I. Khomskii, E. Pellegrin, A. A. Nugroho, A. A. Menovsky, and G. A. Sawatzky, Nature (London) **396**, 441 (1998).
[7] Y. Ren, T. T. M. Palstra, D. I. Khomskii, A. A. Nugroho, A. A. Menovsky, and G. A. Sawatzky, Phys. Rev. B **62**, 6577 (2000).
[8] T. Mizokawa, D. I. Khomskii, and G. A. Sawatzky, Phys. Rev. B **60**, 7309 (1999).
[9] G. R. Blake, T. T. M. Palstra, Y. Ren, A. A. Nugroho, and A. A. Menovsky, Phys. Rev. Lett. **87**, 245501 (2001).
[10] G. R. Blake, T. T. M. Palstra, Y. Ren, A. A. Nugroho, and A. A. Menovsky, Phys. Rev. B **65**, 174112 (2002).
[11] A. A. Tsvetkov, F. P. Mena, P. H. M. van Loosdrecht, D. van der Marel, Y. Ren, A. A. Nugroho, A. A. Menovsky, I. S. Elfimov, and G. A. Sawatzky, Phys. Rev. B **69**, 075110 (2004).
[12] M. Noguchi, A. Nakazawa, S. Oka, T. Arima, Y. Wakabayashi, H. Nakao, and Y. Murakami, Phys. Rev. B **62**, R9271 (2000).
[13] Y. Murakami, H. Kawada, H. Kawata, M. Tanaka, T. Arima, Y. Moritomo, and Y. Tokura, Phys. Rev. Lett. **80**, 1932 (1998).
[14] M. Benfatto, Y. Joly, and C. R. Natoli, Phys. Rev. Lett. **83**, 636 (1999).
[15] M. Takahashi, J.-i. Igarashi, and P. Fulde, J. Phys. Soc. Jpn. **68**, 2530 (1999).
[16] S. B. Wilkins, P. D. Spencer, P. D. Hatton, S. P. Collins, M. D. Roper, D. Prabhakaran, and A. T. Boothroyd, Phys. Rev. Lett. **91**, 167205 (2003).
[17] S. B. Wilkins, N. Stojic, T. A. W. Beale, N. Binggeli, C. W. M. Castleton, P. Bencok, D. Prabhakaran, A. T. Boothroyd, P. D. Hatton, and M. Altarelli, Phys. Rev. B **71**, 245102 (2005).
[18] M. Takahashi and J. I. Igarashi, Phys. Rev. B **65**, 205114 (2002).
[19] Y. Joly, Phys. Rev. B **63**, 125120 (2001).
[20] D. Prabhakaran and A. T. Boothroyd, in *Frontiers in Magnetic Materials*, edited by A. Narlikar (Springer-Verlag, Berlin, 2005), pp. 97–115.
[21] S. B. Wilkins, P. D. Spencer, P. D. Hatton, B. K. Tanner, T. A. Lafford, J. Spence, and N. Loxley, Rev. Sci. Instrum. **73**, 2666 (2002).
[22] S. D. Brown *et al.*, J. Synchrotron Radiat. **8**, 1172 (2001).
[23] L. Paolasini *et al.*, J. Synchrotron Radiat. **14**, 301 (2007).
[24] R. D. Johnson, S. R. Bland, C. Mazzoli, T. A. W. Beale, C. H. Du, C. Detlefs, S. B. Wilkins, and P. D. Hatton, Phys. Rev. B **78**, 104407 (2008).
[25] V. Scagnoli, C. Mazzoli, C. Detelfs, P. Bernard, A. Fondacaro, L. Paolasini, F. Fabrizi, and F. de Bergevin, J. Synchrotron Radiat. **16**, 778 (2009).
[26] M. Renninger, Z. Physik **106**, 141 (1937).
[27] G. Subias, J. Herrero-Martín, J. García, J. Blasco, C. Mazzoli, K. Hatada, S. DiMatteo, and C. R. Natoli, Phys. Rev. B **75**, 235101 (2007).
[28] M. Kanazawa, K. Hagiwara, J. Kokubun, and K. Ishida, J. Phys. Soc. Jpn. **71**, 1765 (2002).
[29] S. R. Bland, B. Detlefs, S. B. Wilkins, T. A. W. Beale, C. Mazzoli, Y. Joly, P. D. Hatton, J. E. Lorenzo, and V. A. M. Brabers, J. Phys.: Condens. Matter **21**, 485601 (2009).
[30] D. H. Templeton and L. K. Templeton, Acta Crystallogr. **A36**, 237 (1980).
[31] V. E. Dmitrienko, K. Ishida, A. Kirfel, and E. N. Ovchinnikova, Acta Crystallogr. **A61**, 481 (2005).
[32] M. H. Sage, G. R. Blake, C. Marquina, and T. T. M. Palstra, Phys. Rev. B **76**, 195102 (2007).
[33] M. Reehuis, C. Ulrich, P. Pattison, B. Ouladdiaf, M. C. Rheinstadter, M. Ohl, L. P. Regnault, M. Miyasaka, Y. Tokura, and B. Keimer, Phys. Rev. B **73**, 094440 (2006).
[34] C. Ulrich, G. Khaliullin, J. Sirker, M. Reehuis, M. Ohl, S. Miyasaka, Y. Tokura, and B. Keimer, Phys. Rev. Lett. **91**, 257202 (2003).
[35] P. Horsch, G. Khaliullin, and A. M. Oleś, Phys. Rev. Lett. **91**, 257203 (2003).
[36] R. V. Yusupov, D. Mihailovic, C. V. Colin, G. R. Blake, and T. T. M. Palstra, Phys. Rev. B **81**, 075103 (2010).
[37] S. D. Matteo, J. Phys.: Conf. Ser. **190**, 012008 (2009).
[38] L. Paolasini *et al.*, Phys. Rev. Lett. **82**, 4719 (1999).
[39] V. E. Dmitrienko, Acta Crystallogr. **A39**, 29 (1983).
[40] M. Blume and D. Gibbs, Phys. Rev. B **37**, 1779 (1988).
[41] C. Mazzoli, S. B. Wilkins, S. Di Matteo, B. Detlefs, C. Detlefs, V. Scagnoli, L. Paolasini, and P. Ghigna, Phys. Rev. B **76**, 195118 (2007).
[42] K. Momma and F. Izumi, J. Appl. Crystallogr. **41**, 653 (2008).